

Carbon–Fluorine Bond Cleavage by Zirconium Metal Hydride Complexes

Brian L. Edelbach, A. K. Fazlur Rahman, Rene J. Lachicotte, and William D. Jones*

Department of Chemistry, University of Rochester, Rochester, New York 14627

Received April 8, 1999

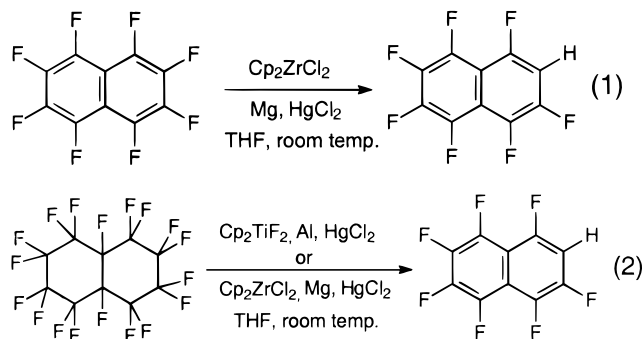
The zirconium hydride dimer $[\text{Cp}_2\text{ZrH}_2]_2$ reacts with C_6F_6 at ambient temperature to give $\text{Cp}_2\text{Zr}(\text{C}_6\text{F}_5)\text{F}$ as the major product along with Cp_2ZrF_2 , $\text{C}_6\text{F}_5\text{H}$ and H_2 . Neither the reaction rate nor the product ratio is affected by changes in H_2 pressure or the concentration of C_6F_6 . The reaction follows zero-order kinetics. The new compound $\text{Cp}_2\text{Zr}(\text{C}_6\text{F}_5)\text{F}$ has been structurally characterized. $[\text{Cp}_2\text{ZrH}_2]_2$ reacts with $\text{C}_6\text{F}_5\text{H}$ to give $\text{Cp}_2\text{Zr}(p\text{-C}_6\text{F}_4\text{H})\text{F}$, Cp_2ZrF_2 , $\text{C}_6\text{F}_4\text{H}_2$, and H_2 . The zirconium hydride Cp_3ZrH has been structurally characterized and also reacts with C_6F_6 . The products of the reaction are CpH , $\text{Cp}_2\text{Zr}(\text{C}_6\text{F}_5)\text{F}$, $\text{C}_6\text{F}_5\text{H}$, Cp_2ZrF_2 , Cp_4Zr , and Cp_3ZrF . The reaction rate is first order in $[\text{Cp}_3\text{ZrH}]$ and $[\text{C}_6\text{F}_6]$, but the product ratio is unaffected by the concentration of C_6F_6 . Possible mechanisms of these reactions are discussed.

Introduction

The use of transition metal complexes to cleave strong carbon–fluorine bonds has blossomed in the past several years.^{1–21} Many late transition metal complexes with electron-donating ligands are believed to undergo oxidative addition to the C–F bond of a fluorinated aromatic group.^{4–9} Catalytic processes for C–F cleavage

have been demonstrated for some of these compounds.^{10–12} Examples of early transition metal complexes that cleave C–F bonds are more rare, perhaps due to the electrophilic nature of the complexes.^{13–16}

Recently, Kiplinger and Richmond provided the first example of selective room-temperature hydrogenolysis of aromatic C–F bonds by homogeneous early transition metal metallocenes.¹⁷ They have shown that octafluoronaphthalene reacts with Cp_2ZrCl_2 in THF with Mg as the terminal reductant to give 1,3,4,5,6,7,8-heptafluoronaphthalene in quantitative yield (eq 1). The C–F bond activation step was proposed to occur via oxidative addition to the transient low-valent zirconocene fragment $[\text{Cp}_2\text{Zr}]$. They have also reported the use of reduced titanocene and zirconocene complexes as catalysts for the aromatization of cyclic perfluorocarbons at room temperature (eq 2).¹⁸



Several prior studies have demonstrated that transition metal hydrides are active for C–F bond cleavage, either by electron transfer¹⁹ or nucleophilic aromatic substitution pathways.²⁰ We have found that the reaction of $[\text{Cp}_2\text{ZrH}_2]_2$ or Cp_3ZrH with perfluorobenzene leads to the formation of the C–F activation product $\text{Cp}_2\text{Zr}(\text{C}_6\text{F}_5)\text{F}$, **1**, as well as Cp_2ZrF_2 and $\text{C}_6\text{F}_5\text{H}$. Evidence is presented that suggests that the C–F cleavage

- (1) Kiplinger, J. L.; Richmond, T. G.; Osterberg, C. E. *Chem. Rev.* **1994**, *94*, 373. Murphy, E. F.; Murugavel, R.; Roesky, H. W. *Chem. Rev.* **1997**, *97*, 3425.
- (2) Burdeniuc, J.; Jedlicka, B.; Crabtree, R. H. *Chem. Ber./Recl.* **1997**, *130*, 145.
- (3) Richmond, T. G. In *Topics in Organometallic Chemistry, Activation of Unreactive Bonds and Organic Synthesis*; Springer-Verlag: New York, 1999; Vol. 3, pp 243–269.
- (4) Belt, S. T.; Helliwell, M.; Jones, W. D.; Partridge, M. G.; Perutz, R. N. *J. Am. Chem. Soc.* **1993**, *115*, 1429.
- (5) Jones, W. D.; Partridge, M. G.; Perutz, R. N. *J. Chem. Soc., Chem. Commun.* **1991**, 264.
- (6) Hofmann, P.; Unfried, G. *Chem. Ber.* **1992**, *125*, 659.
- (7) Lucht, B. L.; Poss, M. J.; King, M. A.; Richmond, T. G. *J. Chem. Soc., Chem. Commun.* **1991**, 400.
- (8) Crespo, M.; Martinez, M.; Sales, J. J. *J. Chem. Soc., Chem. Commun.* **1992**, 822.
- (9) Cronin, L.; Higgitt, C. L.; Karch, R.; Perutz, R. N. *Organometallics* **1997**, *16*, 4920.
- (10) Kiplinger, J. L.; Richmond, T. G. *J. Am. Chem. Soc.* **1996**, *118*, 1805.
- (11) Aizenberg, M.; Milstein, D. *J. Am. Chem. Soc.* **1995**, *117*, 8674.
- (12) Aizenberg, M.; Milstein, D. *Science* **1994**, *265*, 359.
- (13) Burns, C. J.; Andersen, R. A. *J. Chem. Soc., Chem. Commun.* **1989**, 136.
- (14) Watson, P. L.; Tulip, T. H.; Williams, I. *Organometallics* **1990**, *9*, 1999.
- (15) Weydert, M.; Andersen, R. A.; Bergman, R. G. *J. Am. Chem. Soc.* **1993**, *115*, 8837.
- (16) Burk, M. J.; Staley, D. L.; Tumas, W. *J. Chem. Soc., Chem. Commun.* **1990**, 809.
- (17) Kiplinger, J. L.; Richmond, T. G. *J. Am. Chem. Soc. Chem.* **1996**, *118*, 1805.
- (18) Kiplinger, J. L.; Richmond, T. G. *J. Chem. Soc. Commun.* **1996**, 1115.
- (19) Whittlesey, M. K.; Perutz, R. N.; Moore, M. H. *Chem. Commun.* **1997**, *119*, 7734.
- (20) Edelbach, B. L.; Jones, W. D. *J. Am. Chem. Soc.* **1997**, *119*, 7734.
- (21) Hughes, R. P.; Lindner, D. C.; Rheingold, A. L.; Liable-Sands, L. M. *J. Am. Chem. Soc.* **1997**, *119*, 11544.

occurs via a σ -bond metathesis pathway and by way of oxidative addition to $[\text{Cp}_2\text{Zr}]$.

Results

Thermal Reactions of $[\text{Cp}_2\text{ZrH}_2]_2$ with Polyfluorinated Arenes. The thermolysis of $[\text{Cp}_2\text{ZrH}_2]_2$ with 12 equiv of C_6F_6 at 65 °C in THF solution leads to the rapid formation (~ 1 min) of the C–F activated product $\text{Cp}_2\text{Zr}(\text{C}_6\text{F}_5)\text{F}$, **1**, as the major product (80%) as well as smaller quantities of Cp_2ZrF_2 , $\text{C}_6\text{F}_5\text{H}$, and H_2 . The compound $[\text{Cp}_2\text{ZrH}_2]_2$ is only sparingly soluble in THF, but its solution NMR spectrum has been reported and is consistent with a $[\text{Cp}_2\text{Zr}(\text{H})(\mu\text{-H})_2]$ structure.²² The amount of hydrogen released in the reaction was not quantified, but H_2 is clearly seen in a ^1H NMR spectrum of the reaction solution at δ 4.54 (THF- d_8). Good mass balance is observed in accordance with the reaction shown in eq 3. When the reaction is monitored at room



temperature, the product ratios are identical to those at 65 °C, and the product ratio is constant throughout the course of the reaction. The thermolysis of $[\text{Cp}_2\text{ZrD}_2]_2$ with C_6F_6 at 65 °C in THF solution leads to compound **1**, $\text{C}_6\text{F}_5\text{D}$ (as identified by ^{19}F NMR spectroscopy and GC/MS), and Cp_2ZrF_2 in a ratio of 3.5:2.0:1, respectively. The evolution of a gas (presumably D_2) was also observed during the course of the reaction.

The ^1H NMR spectrum of **1** in THF- d_8 was characterized by a single Cp resonance at δ 6.405. The ^{19}F NMR spectrum exhibits a downfield resonance at δ 168.2 corresponding to the zirconium-bound fluoride as well as three distinct upfield resonances in a 2:1:2 ratio at δ –49.3, –93.8, and –98.8, which correspond to the ortho, para, and meta aromatic fluorine resonances, respectively. The meta fluorine resonance is broad, whereas the para and ortho resonances are sharp. The presence of only three aromatic fluorine resonances indicates rapid rotation around the Zr–aryl bond on the NMR time scale at room temperature. A ^{19}F NMR spectrum of **1** at –50 °C exhibits five distinct resonances. The coalescence temperature for both the ortho and meta fluorines is approximately –15 °C. The rate constant at coalescence is 600 s^{-1} for both types of fluorine, corresponding to a barrier to rotation of approximately 11.8 kcal/mol.

A single-crystal X-ray structure of **1** is shown in Figure 1. The complex displays the expected geometry with the C_6F_5 group in the equatorial plane of the $\text{Cp}_2\text{-Zr}$ fragment. The Zr–F bond length of 1.946(2) Å is similar to that seen in Cp_2ZrF_2 (1.98 Å).²³ The Zr–C bond distance of 2.346 Å compares with that of 2.329 Å seen in the only other structurally characterized perfluorophenyl zirconium complex, $[(\text{Cp})[\eta\text{-CPh}\{\text{N}(\text{SiMe}_3)_2\}](\text{C}_6\text{F}_5)\text{Zr}\{\mu\text{-MeB}(\text{C}_6\text{F}_5)_3\}]$.²⁴

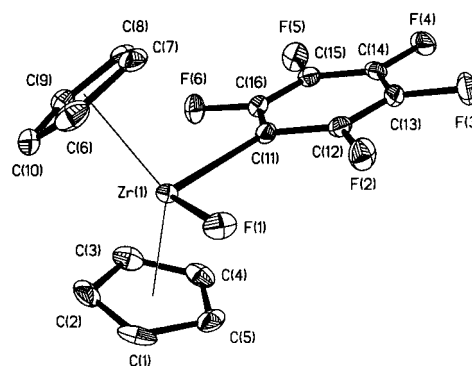


Figure 1. ORTEP drawing of **1** showing 30% probability ellipsoids.

The effect of solvent on the reaction rate and ratio of products was tested by performing the same reaction in *p*-xylene- d_{10} , CD_2Cl_2 , and pyridine- d_5 . The reaction in *p*-xylene- d_{10} gave the same product ratios as that in THF; however the rate is approximately one-tenth as fast. The reaction in CD_2Cl_2 gives Cp_2ZrCl_2 as the main organometallic complex. No **1**, $\text{C}_6\text{F}_5\text{H}$, or Cp_2ZrF_2 is observed. When the reaction is run in pyridine, the product ratio is 7.4:1:1.4 for **1**, $\text{C}_6\text{F}_5\text{H}$, and Cp_2ZrF_2 , respectively. A large broad singlet at δ 102 was also observed but not identified (we determined it was not pyridine·HF by adding 1 μL of pyridinium poly(hydrogen fluoride) ($\sim 30\%$ pyridine/70% hydrogen fluoride) to an NMR tube containing 0.5 mL of pyridine).

Free radical intermediates can be virtually ruled out in these reactions. When the thermal reaction of $[\text{Cp}_2\text{-ZrH}_2]_2$ with C_6F_6 was carried out in the presence of the radical trap 9,10-dihydroanthracene (10 equiv) in THF, the rate of reaction and product ratios were not affected. The same results were observed when the reaction was run in neat isopropylbenzene as trap and the reaction monitored by ^{19}F NMR spectroscopy. Also, the use of $[\text{Cp}_2\text{ZrH}_2]_2$ prepared from the reaction of Cp_2ZrMe_2 with H_2 produced identical product distributions.

The rate and ratio of product formation shown in eq 3 is unaffected by the pressure of H_2 (0 vs 4 atm of H_2) or the concentration of C_6F_6 . When the reaction is performed in a sealed NMR tube at room temperature with varying concentrations of C_6F_6 (0.88, 1.78, and 2.68 M), the appearance of **1** follows zero-order kinetics (Figure 2). That is, a plot of **[1]** vs time is linear, suggesting that the rate is limited by the rate of dissolving of $[\text{Cp}_2\text{ZrH}_2]_2$ or that the solution is saturated in $[\text{Cp}_2\text{ZrH}_2]_2$ and the rate is determined by the rate of cleavage of $[\text{Cp}_2\text{ZrH}_2]_2$ into Cp_2ZrH_2 . The rate of disappearance of $[\text{Cp}_2\text{ZrH}_2]_2$ was seen to depend on the rate of stirring. An unstirred sample of $[\text{Cp}_2\text{ZrH}_2]_2$ containing C_6F_6 reacts much more slowly than a stirred sample containing the same concentration of C_6F_6 (Figure 2), indicating that mass transport is rate limiting.

Various zirconocene, $[\text{Cp}_2\text{Zr}]$, synthons were reacted with C_6F_6 to determine if formal oxidative addition of $[\text{Cp}_2\text{Zr}]$ to the aromatic carbon–fluorine bond to form complex **1** was viable. The complexes $\text{Cp}_2\text{Zr}(\text{CH}_2=\text{CH}\text{Et})$ and $\text{Cp}_2\text{Zr}(\text{CH}_2=\text{CH}_2)$ generated in situ from Cp_2ZrBu_2 and Cp_2ZrEt_2 , respectively, are known to act as $[\text{Cp}_2\text{-Zr}]$ equivalents.²⁵ Recently, it has been demonstrated

(22) Bickley, D. G.; Hao, N.; Bougeard, P.; Sayer, B. G.; Burns, R. C.; McGlinchey, M. J. *J. Organomet. Chem.* **1983**, 246, 257.

(23) Bush, M. A.; Sim, G. A. *J. Chem. Soc. (A)* **1971**, 2225.

(24) Gomez, R.; Green, M. L. H.; Haggitt, J. L. *J. Chem. Soc., Chem. Commun.* **1994**, 2607.

(25) Negishi, E.; Takahashi, T. *Bull. Chem. Soc. Jpn.* **1998**, 755, 5–769, and references therein.

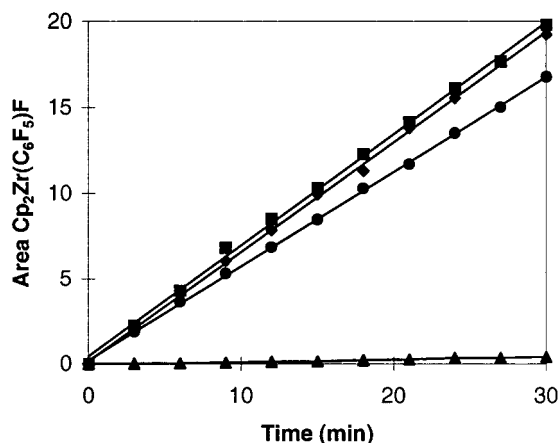


Figure 2. Graph of appearance of $\text{Cp}_2\text{Zr}(\text{C}_6\text{F}_5)\text{F}$ vs time (min): \bullet = 0.88 M C_6F_6 with stirring, \blacksquare = 1.78 M C_6F_6 with stirring, \blacklozenge = 2.68 M C_6F_6 with stirring, \blacktriangle = 1.78 M C_6F_6 without stirring.

that the complex $\text{Cp}_2\text{Zr}(\text{Me}_3\text{SiC}\equiv\text{CSiMe}_3)(\text{THF})$ can also serve as a $[\text{Cp}_2\text{Zr}]$ equivalent.²⁶ Reaction of any of these complexes with C_6F_6 in THF- d_8 leads to decomposition rather than formation of **1**.

The thermal reaction of $[\text{Cp}_2\text{ZrH}_2]_2$ with 12 equiv of $\text{C}_6\text{F}_5\text{H}$ at 65 °C in THF solution leads to the formation of the C–F activation product $\text{Cp}_2\text{Zr}(p\text{-C}_6\text{F}_4\text{H})\text{F}$ as the major product as well as Cp_2ZrF_2 , $\text{C}_6\text{F}_4\text{H}_2$, and H_2 in the same ratios as observed in the reaction with C_6F_6 . The complex $\text{Cp}_2\text{Zr}(\text{C}_6\text{F}_5)\text{H}$, arising from C–H activation of $\text{C}_6\text{F}_5\text{H}$, was not observed. The ^1H NMR spectrum of $\text{Cp}_2\text{Zr}(p\text{-C}_6\text{F}_4\text{H})\text{F}$ was characterized by a single Cp resonance at δ 6.40 in THF- d_8 , as well as an aromatic resonance at δ 7.027 (tt, $J_{\text{H-F}} = 9.4, 7.1$ Hz). The triplet of triplets pattern is consistent with a hydrogen coupling to two ortho and two meta fluorines, indicating that C–F activation occurred exclusively para to the hydrogen in $\text{C}_6\text{F}_5\text{H}$. The ^{19}F NMR spectrum exhibits a downfield resonance at δ 166.2 corresponding to the zirconium-bound fluoride as well as two broad upfield resonances in a 1:1 ratio at δ –51.6, –76.3, which correspond to the ortho and meta aromatic fluorines, respectively. The presence of only two aromatic fluorine resonances indicates rapid rotation around the Zr–aryl bond on the NMR time scale at room temperature. A ^{19}F NMR spectrum of $\text{Cp}_2\text{Zr}(p\text{-C}_6\text{F}_4\text{H})\text{F}$ at –70 °C exhibits four distinct resonances. The coalescence temperature is approximately –15 °C for the meta fluorine and approximately –30 °C for the ortho fluorines. The rate constants at coalescence are 476 and 184 s^{-1} for the meta fluorine and ortho fluorines, respectively, which correspond to a barrier to rotation of approximately 11.4 kcal/mol.

In an attempt to synthesize possible intermediates, such as Cp_2ZrHF , pyridinium poly(hydrogen fluoride) was added to $[\text{Cp}_2\text{ZrH}_2]_2$ in THF. The addition of 2 equiv of pyridinium poly(hydrogen fluoride) per Zr atom leads to quantitative formation of Cp_2ZrF_2 (hydrogen gas was also observed). Addition of 1 equiv of pyridinium poly(hydrogen fluoride) per Zr atom also leads to Cp_2ZrF_2 , with unreacted $[\text{Cp}_2\text{ZrH}_2]_2$ remaining in the reaction flask. Although Cp_2ZrHF is a likely intermediate in this

reaction, it must rapidly disproportion to give Cp_2ZrF_2 and Cp_2ZrH_2 .

Structure of Cp_3ZrH . The synthesis of the complex Cp_3ZrH (**2**) was reported in 1981 by the reaction of Cp_4Zr and LiAlH_4 .²⁷ Andersen has also reported an improved synthesis of the complex by reaction of Cp_4Zr with $t\text{-BuLi}$.²⁸ This complex might formally be assigned a $20 e^-$ configuration should all Cp rings be η^5 -coordinate, but it has been pointed out that the lack of a metal orbital with a_2' symmetry prevents bonding with the corresponding group orbital on the three cyclopentadienyl ligands, so that one pair of electrons from the Cp_3 donor set cannot be included in the metal's electronic configuration.²⁹ While no X-ray structure for **2** has been reported, IR studies indicated that all three Cp ligands were η^5 -coordinated.³⁰

We have found that colorless **2** crystallizes in trigonal space group $P6_3/m$ with $Z = 2$, consistent with a molecule of **2** being disordered on a $3/m (=6)$ center. Solution and initial refinement of the Cp_3Zr portion of the molecule showed residual electron density that could be associated with the hydride ligand approximately 2 Å from the Zr on the $3/m$ center. Furthermore, the anisotropic thermal ellipsoid for the Zr showed substantial elongation along the 3-fold axis. A different model was introduced in which half of a Zr was introduced 0.3 Å away from the mirror plane but on the 3-fold axis. The improved refinement along with the isotropic appearance of the Zr thermal ellipsoid indicated that this model was superior. Furthermore, the hydride ligand could now be refined, also disordered over either side of the mirror plane. In the final model, the positions and thermal parameters of all atoms were refined, with the hydrogen atoms being refined isotropically. The Zr lies 0.20 Å away from the mirror plane, and the Zr–H distance is 1.72(10) Å. Other Cp_3ZrX molecules that have been structurally characterized also show Zr to be away from the plane of the three Cp centroids.³¹

Andersen has reported the synthesis and structure of the related Zr^{III} species, Cp_3Zr .²⁸ Crystals of this d^1 complex are brown, and the molecule crystallizes in the same space group as **2**. Furthermore, the coordinates reported for Cp_3Zr are virtually identical to those found for **2**, with one important difference in the refinement. The model placed the zirconium at the $3/m$ center, on the mirror plane. The thermal ellipsoid for Zr is elongated along the 3-fold axis, but only slightly. Consequently, it appears that the Cp_3Zr core of **2** is isomorphous and nearly isostructural with Cp_3Zr . When the model for **2** was modified to place the Zr on the

(27) Brainina, E. M.; Strunkina, L. I.; Lokshin, B. V.; Ezernitskaya, M. G. *Izv. Akad. Nauk SSSR, Ser. Khim.* **1981**, 447.

(28) Lukens, W. W.; Andersen, R. A. *Organometallics* **1995**, *14*, 3435.

(29) (a) Bursten, B. E.; Rhodes, L. F.; Strittmatter, R. J. *J. Am. Chem. Soc.* **1989**, *111*, 2756. (b) Strittmatter, R. J.; Bursten, B. E. *J. Am. Chem. Soc.* **1991**, *113*, 552. (c) Lauher, J. W.; Hoffman, R. J. *J. Am. Chem. Soc.* **1976**, *98*, 1729.

(30) Lokshin, B. V.; Klemenkova, Z. S.; Ezernitskaya, M. G.; Strunkina, L. I.; Brainina, E. M. *J. Organomet. Chem.* **1982**, *235*, 69.

(31) (a) Brackmeyer, T.; Erker, G.; Fröhlich, R. *Organometallics* **1997**, *16*, 531. (b) Rogers, R. D.; Bynum, R. V.; Atwood, J. L. *J. Am. Chem. Soc.* **1978**, *100*, 5238. (c) Ushioda, T.; Green, M. L. H.; Haggitt, J.; Yan, X. *J. Organomet. Chem.* **1996**, *518*, 155. (d) Kulishov, V. I.; Bokii, N. G.; Struchkov, Y. T. *Zh. Strukt. Khim.* **1970**, *11*, 700. (e) Kopf, J.; Vollmer, H. J.; Kaminsky, W. *Cryst. Struct. Commun.* **1980**, *9*, 985. (f) Diamond, G. M.; Green, M. L. H.; Popham, N. A.; Chernega, A. N. *J. Chem. Soc., Dalton Trans.* **1993**, 2535. (g) Brackmeyer, T.; Erker, G.; Fröhlich, R.; Prigge, U.; Peuchert, U. *Chem. Ber.* **1997**, *130*, 899.

(26) Ohff, A.; Pulst, S.; Lefebvre, C.; Peulecke, N.; Arndt, P.; Burlakov, V. V.; Rosenthal, U. *Synlett* **1996**, 111.

mirror plane and the hydride omitted (as if it were Cp_3Zr), refinement showed a severely elongated thermal ellipsoid for Zr, indicating the incorrectness of this model (see Supporting Information).

Thermal Reactions of Cp_3ZrH with C_6F_6 . The complex Cp_3ZrH , **2**, is also capable of cleaving the C–F bond of C_6F_6 at room temperature. The major products of the reaction are **1** and CpH , formed in equimolar quantities, which account for 55% of the total yield based upon Cp_3ZrH . Minor products observed include Cp_2ZrF_2 (14%), Cp_4Zr (11%), $\text{C}_6\text{F}_5\text{H}$ (38%), and the new compound Cp_3ZrF (11%). The rate of the reaction showed a first-order dependence on the concentration of C_6F_6 . As in the reaction of $[\text{Cp}_2\text{ZrH}_2]_2$, the product ratio is unaffected by the concentration of C_6F_6 or by addition of CpH .

The complex assigned as Cp_3ZrF can be produced independently by addition of 0.5 equiv of pyridinium poly(hydrogen fluoride) to Cp_4Zr . Free cyclopentadiene, Cp_3ZrF , and Cp_2ZrF_2 are formed, the latter two in a 1.8:1 ratio. The new compound Cp_3ZrF was characterized by ^1H and ^{19}F NMR spectroscopy, as well as mass spectroscopy. The ^1H NMR spectrum of Cp_3ZrF in $\text{THF}-d_8$ consists of a single Cp resonance at δ 6.099, and the ^{19}F NMR spectrum exhibits one distinct resonance at δ 25.5. Direct inlet MS shows a peak at m/e 304 for M^+ , as well as fragments at 285 ($\text{M}^+ - \text{F}$) and 239 ($\text{M}^+ - \text{Cp}$, 100%).

Previously, we reported that the addition of fluoride (via tetrabutylammonium fluoride, TBAF) to a solution containing $(\text{C}_5\text{Me}_5)\text{Rh}(\text{PMe}_3)_2\text{H}_2$ and C_6F_6 greatly accelerated the formation $(\text{C}_5\text{Me}_5)\text{Rh}(\text{PMe}_3)(\text{C}_6\text{F}_5)\text{H}$.²⁰ It was demonstrated that fluoride acted as a base by deprotonating $(\text{C}_5\text{Me}_5)\text{Rh}(\text{PMe}_3)_2\text{H}_2$ to give $[(\text{C}_5\text{Me}_5)\text{Rh}(\text{PMe}_3)\text{H}]^-$, which undergoes nucleophilic aromatic substitution with C_6F_6 to give $(\text{C}_5\text{Me}_5)\text{Rh}(\text{PMe}_3)(\text{C}_6\text{F}_5)\text{H}$. An analogous reaction was performed by adding TBAF (~ 1.4 equiv) to a solution containing Cp_3ZrH and C_6F_6 . No rate acceleration was observed, and the main product in the reaction was Cp_2ZrF_2 .

Discussion

Mechanistic Considerations for the Reaction of $[\text{Cp}_2\text{ZrH}_2]_2$ with C_6F_6 . One possible mechanism for the formation of the products depicted in eq 3 is a concerted σ -bond metathesis in which the aryl^F carbon of C_6F_6 bonds to the zirconium and the fluorine bonds to the hydride (Figure 4). The products of this reaction are $\text{Cp}_2\text{Zr}(\text{C}_6\text{F}_5)\text{H}$ and HF. Hydrogen fluoride could then protonate the Zr–H bond of $\text{Cp}_2\text{Zr}(\text{C}_6\text{F}_5)\text{H}$ to give **1** and H_2 or protonate the Zr– C_6F_5 bond to give Cp_2ZrHF and $\text{C}_6\text{F}_5\text{H}$. The complex Cp_2ZrHF conproportionates to give Cp_2ZrF_2 and Cp_2ZrH_2 . While this mechanism accounts for all of the observed products, it has several drawbacks. First, given the crowded environment shown in Figure 4 and the strong fluorophilicity of zirconium, metathesis in the opposite direction should be favored (vide infra). Second, the addition of Proton-Sponge³² had no effect on the rate or the products formed in the reaction, and no pyridinium HF was observed when the

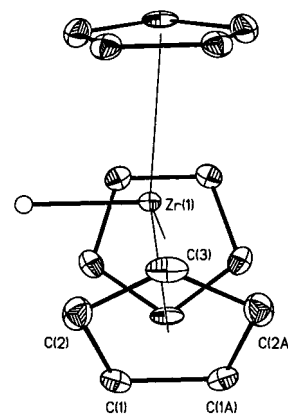


Figure 3. ORTEP drawing of **2** showing 30% probability ellipsoids. Cp-hydrogens have been omitted for clarity.

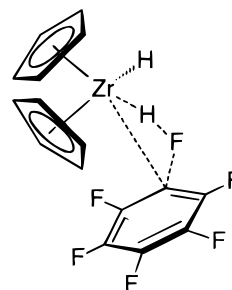
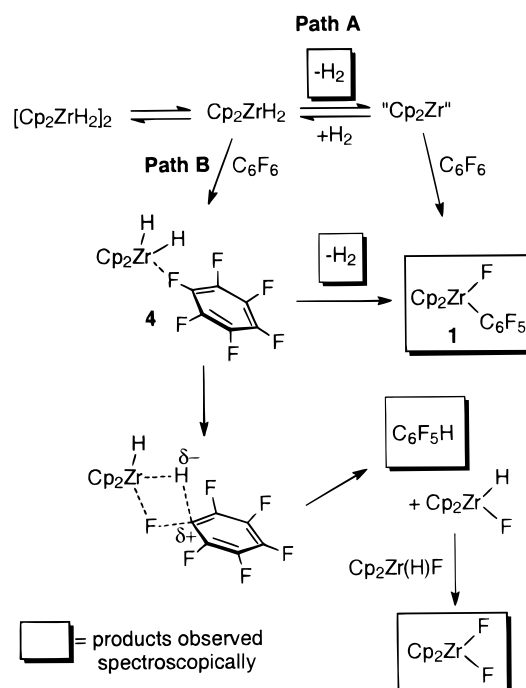


Figure 4. Possible transition state for C–F activation.

Scheme 1. Possible Mechanisms for the Reaction of $[\text{Cp}_2\text{ZrH}_2]_2$ with C_6F_6



reaction was run in pyridine. Both of these observations suggest that HF is not formed during the course of the reaction.

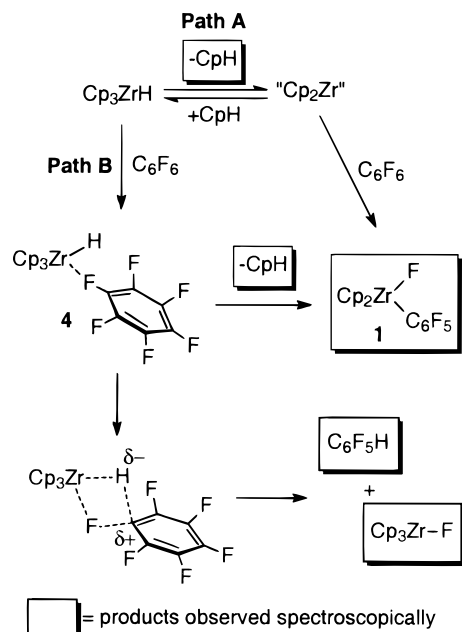
Two other mechanistic pathways are depicted in Scheme 1. Both paths involve initial dimer cleavage to monomer. In path A this is followed by loss of H_2 from the monomer to give $[\text{Cp}_2\text{Zr}]$, which then undergoes a formal oxidative addition to C_6F_6 to give compound **1**. To our knowledge, thermal reductive elimination of H_2

(32) Proton Sponge is a trademark name for [1,8-bis(dimethylamino)naphthalene, N,N,N',N' -tetramethyl-1,8-naphthalenediamine], $\text{C}_{10}\text{H}_{16}[\text{N}(\text{CH}_3)_2]_2$.

from Cp_2ZrH_2 has not been reported. Path A can be ruled out as the exclusive pathway since it does not account for the formation of $\text{C}_6\text{F}_5\text{H}$ or Cp_2ZrF_2 . Path A can also be ruled out as a competing pathway for the formation of **1** based on the following argument. Neither the pressure of H_2 nor the concentration of C_6F_6 had an effect on the product ratios. If path A is contributing to the formation of **1**, the *product ratio* should change with changes in H_2 pressure (if reaction of $[\text{Cp}_2\text{Zr}]$ with C_6F_6 is rate determining in path A) or with changes in the concentration of C_6F_6 (if loss of H_2 from Cp_2ZrH_2 is rate determining in path A). The fact that no effect upon *product ratio* was observed with changes in the amount of H_2 or C_6F_6 present appears to rule out path A altogether.

In path B an interaction is depicted between the fluorophilic Zr(IV) center on Cp_2ZrH_2 and a fluorine on C_6F_6 to give complex **4** (Scheme 1). The interaction of aromatic C–F bonds with bis(cyclopentadienyl) Zr(IV) type species has been reported,³³ and several of these complexes have been characterized by X-ray crystallography.^{33b,c,d} Erker et al. have estimated the C–F...Zr bond dissociation energy in the $(\text{CH}_3\text{C}_5\text{H}_4)_2\text{Zr}(\mu\text{-C}_4\text{H}_6)\text{B}(\text{C}_6\text{F}_5)_3$ betaine complex at approximately 8–9 kcal/mol.^{33c} In the reaction of Cp_2ZrH_2 and C_6F_6 this interaction results in two possible reactivity patterns. First, the Zr...F–(C₆F₅) association may result in an associatively induced reductive elimination of H_2 from Cp_2ZrH_2 to give $[\text{Cp}_2\text{Zr} \cdots \text{F}(\text{C}_6\text{F}_5)]$, which then undergoes a formal oxidative addition to C_6F_6 to give compound **1**. In a similar pathway, Schwartz et al. have shown that reductive elimination of methane from $\text{Cp}_2\text{Zr}(\text{Me})(\text{H})$ involves initial coordination of a 2e donor ligand.³⁴ Other examples involving ligand-induced reductive elimination from late transition metals have also been reported.³⁵ In a second competing pathway, a concerted σ -bond metathesis occurs, resulting in the formation of $\text{C}_6\text{F}_5\text{H}$ and Cp_2ZrHF , which conproportionates to give Cp_2ZrF_2 and Cp_2ZrH_2 (Scheme 1). Metathesis in this direction is facilitated by attack of the hydridic proton on the aromatic carbon of C_6F_6 and by the strong fluorophilicity of zirconium. The nucleophilicity of the hydrogens on Cp_2ZrH_2 has been well established,³⁶ and nucleophilic attack on polyfluorinated aromatic rings is well documented. This later reaction sequence accounts for the fact that only 0.5 mol of Cp_2ZrF_2 is observed for every mole of $\text{C}_6\text{F}_5\text{H}$ produced. Finally, the small observed isotope effect suggests that Zr–H(D) bond cleavage is occurring before or during the rate-determining step.

Scheme 2. Possible Mechanisms for the Reaction of Cp_3ZrH with C_6F_6



One might argue against the mechanism depicted in path B based on the observation that all of the $[\text{Cp}_2\text{Zr}]$ synthons employed failed to give compound **1**. However, a detailed study on the chemistry of the $\text{Cp}_2\text{ZrCl}_2/2 n\text{-BuLi}$ system has demonstrated that the thermal decomposition of the resulting dibutylzirconocene results in a myriad of intermediates and casts doubt that this system or other related systems truly lead to a simple $[\text{Cp}_2\text{Zr}]$ synthon.³⁷

Mechanistic Considerations for the Reaction of Cp_3ZrH with C_6F_6 . Two mechanisms for the reaction of Cp_3ZrH with C_6F_6 are outlined in Scheme 2. Both are analogous to those presented in the $[\text{Cp}_2\text{ZrH}_2]_2$ system. Path A involves reversible reductive elimination of free CpH to give the putative 14-electron $[\text{Cp}_2\text{Zr}]$ fragment, which cleaves the C–F bond of C_6F_6 to give compound **1**. Path A is again ruled out due to lack of change in product ratio with changes in C_6F_6 concentration or addition of CpH.

Path B depicts a C–F...Zr interaction between C_6F_6 and Cp_3ZrH , as suggested above. This interaction may lead to an associatively induced reductive elimination of CpH and C–F bond activation of C_6F_6 by the $[\text{Cp}_2\text{Zr} \cdots \text{F}(\text{C}_6\text{F}_5)]$ intermediate to give complex **1**. This pathway accounts for the 1:1 ratio of CpH to **1** observed in the overall reaction. The same interaction may also lead to a σ -bond metathesis between Cp_3ZrH and C_6F_6 to give $\text{C}_6\text{F}_5\text{H}$ and Cp_3ZrF . This pathway should result in a 1:1 ratio of $\text{C}_6\text{F}_5\text{H}$ to Cp_3ZrF . In contrast, the observed ratio of $\text{C}_6\text{F}_5\text{H}$ to Cp_3ZrF is ~2.7:1. The deficiency of Cp_3ZrF can be accounted for by the observation of the small quantities of Cp_2ZrF_2 and Cp_4Zr , in terms of mass balance. Path B is also consistent with the observed first-order decay of Cp_3ZrH in the reaction with C_6F_6 , assuming the reaction of Cp_3ZrH with C_6F_6 is the slow step. Reaction of **2** with C_6F_6 in the presence of 0.79 M cumene gives an almost identical mixture of products, ruling out radical processes.

(33) (a) Horton, A. D.; Orpen, A. G. *Organometallics* **1991**, *10*, 3910. (b) Yang, X.; Stern, C. L.; Marks, T. J. *J. Am. Chem. Soc.* **1994**, *116*, 10015. (c) Karl, J.; Erker, G.; Fröhlich, R. *J. Am. Chem. Soc.* **1997**, *119*, 11165. (d) Dahlmann, M.; Erker, G.; Nissinen, M.; Fröhlich, R. *J. Am. Chem. Soc.* **1999**, *121*, 2820. (e) Watson, P. L.; Tulip, T. H.; Williams, I. *Organometallics* **1990**, *9*, 1999. (f) Lancaster, S. J.; Thornton-Pett, M.; Dawson, D. M.; Bochmann, M. *Organometallics* **1998**, *17*, 3829.

(34) (a) Gell, K. I.; Schwartz, J. J. *J. Am. Chem. Soc.* **1978**, *100*, 3246. (b) Gell, K. I.; Schwartz, J. J. *J. Am. Chem. Soc.* **1981**, *103*, 2687.

(35) (a) Abis, L.; Sen, A.; Halpern, J. *J. Am. Chem. Soc.* **1978**, *100*, 2915. (b) Jones, W. D.; Hessel, E. T. *J. Am. Chem. Soc.* **1992**, *114*, 6087. (c) Yamamoto, T.; Abila, M. *J. Organomet. Chem.* **1997**, *535*, 209. (d) Wick, D. D.; Reynolds, K. A.; Jones, W. D. *J. Am. Chem. Soc.* **1999**, *121*, 3974.

(36) (a) Labinger, J. A.; Komadina, J. H. *J. Organomet. Chem.* **1978**, *155*, C25. (b) Labinger, J. A. In *Transition Metal Hydrides*; Dedieu, A., Ed.; VCH: New York, 1992; Chapter 10.

(37) Dioumaev, V. K.; Harrod, J. F. *Organometallics* **1997**, *16*, 1452.

Conclusions

The zirconium hydrides $[\text{Cp}_2\text{ZrH}_2]_2$ and Cp_3ZrH react with C_6F_6 to give the C–F activation product $\text{Cp}_2\text{Zr}(\text{C}_6\text{F}_5)\text{F}$. Mechanistic studies are consistent with an initial association between the zirconium metal center and C_6F_6 via fluorine. Such an interaction may lead to ligand-assisted loss of H_2 or (CpH) and C–F activation, resulting in the formation of a zirconium–fluorine bond. Competitively, a σ -bond metathesis between the zirconium hydride and C_6F_6 may also occur, resulting in the formation of a new zirconium fluoride complex and a new C–H bond. A similar mechanism is also postulated for the Cp_3ZrH system. Further studies are under way with the more soluble $(\text{C}_5\text{Me}_5)\text{ZrH}_2$ system in order to gain more insight into the mechanism of these reactions.

Experimental Section

General Considerations. All manipulations were performed under an N_2 atmosphere, either on a high-vacuum line using modified Schlenk techniques or in a Vacuum Atmospheres Corporation glovebox. Tetrahydrofuran, benzene, ether, and toluene were distilled from dark purple solutions of benzophenone ketyl. Alkane solvents were made olefin-free by stirring over H_2SO_4 , washing with aqueous KMnO_4 and water, and distilling from dark purple solutions of tetraglyme/benzophenone ketyl. Benzene- d_6 , p -xylene- d_{10} , and tetrahydrofuran- d_8 were purchased from Cambridge Isotope Laboratories, distilled under vacuum from dark purple solutions of benzophenone ketyl, and stored in ampules with Teflon sealed vacuum line adapters. CD_2Cl_2 was purchased from Cambridge Isotope Laboratories and distilled under vacuum from a solution of calcium hydride. Pyridine was dried with calcium hydride and stored over molecular sieves. The preparations of $\text{C}_6\text{F}_5\text{Li}$,³⁸ $[\text{Cp}_2\text{ZrH}_2]_2$,³⁹ Cp_3ZrH ,²⁸ Cp_2ZrF_2 ,⁴⁰ Cp_4Zr ,⁴¹ $\text{Cp}_2\text{Zr}(\text{C}_6\text{F}_5)_2$,⁴² and “anhydrous TBAF”²⁰ have been previously reported. Pyridinium poly(hydrogen fluoride) (~30% pyridine/70% hydrogen fluoride), Proton Sponge, and the fluorinated aromatic compounds were purchased from Aldrich Chemical Co. The liquids were stirred over sieves, freeze–pump–thaw degassed three times, and vacuum distilled prior to use.

All ^1H NMR and ^{19}F NMR spectra were recorded on a Bruker Avance 400 spectrometer. All ^1H chemical shifts are reported in ppm (δ) relative to tetramethylsilane and referenced using chemical shifts of residual solvent resonances (THF- d_8 , δ 1.73). ^{19}F NMR spectra were referenced to external $\text{C}_6\text{H}_5\text{CF}_3$ (δ 0.00 with downfield chemical shifts taken to be positive; CFCl_3 appears at δ +62.54 relative to internal $\text{C}_6\text{H}_5\text{CF}_3$ in THF- d_8 solvent). GC–MS was conducted on a 5890 Series II gas chromatograph fitted with an HP 5970 series mass selective detector. Analyses were obtained from Desert Analytics. A Siemens SMART system with a CCD area detector were used for X-ray structure determination. Kinetic fits were performed using Microsoft Excel. All errors are quoted as 95% confidence limits (\pm error = $t\sigma$, σ = standard deviation, t from student's t -distribution).

Thermolysis of $[\text{Cp}_2\text{ZrH}_2]_2$ with Perfluorobenzene. A sample of $[\text{Cp}_2\text{ZrH}_2]_2$ (244 mg, 0.546 mmol) was suspended in 8 mL of THF. Perfluorobenzene (13.1 mmol, 1.5 mL) was added at room temperature, and the mixture was heated to 65 °C.

Within a few minutes vigorous gas evolution was observed and the suspension of $[\text{Cp}_2\text{ZrH}_2]_2$ disappeared to give a clear colorless solution. The solvent, excess C_6F_6 , $\text{C}_6\text{F}_5\text{H}$, and H_2 were removed under vacuum to give a white powder (412 mg). A ^1H NMR spectrum of the sample revealed a 4:1 mixture of $\text{Cp}_2\text{Zr}(\text{C}_6\text{F}_5)\text{F}$, **1**, and Cp_2ZrF_2 . Compound **1** can be separated from Cp_2ZrF_2 by dissolving the mixture in a minimum of THF and layering with hexanes. X-ray quality crystals of **1** are formed with Cp_2ZrF_2 remaining in solution. An NMR tube scale reaction was performed at 65 °C with 14.5 mg (0.065 mmol based on monomer) of $[\text{Cp}_2\text{ZrH}_2]_2$ and C_6F_6 (0.84 mmol, 97 μL) in THF- d_8 . Integration revealed a 6:1:2 mixture of $\text{Cp}_2\text{Zr}(\text{C}_6\text{F}_5)\text{F}$, Cp_2ZrF_2 , and $\text{C}_6\text{F}_5\text{H}$, respectively. Hydrogen is also observed at δ 4.55 ppm. The formation of zirconium species was quantitative. For $\text{Cp}_2\text{Zr}(\text{C}_6\text{F}_5)\text{F}$, ^1H NMR (THF- d_8): δ 6.405 (s, 10 H). ^{19}F NMR (THF- d_8 , 23 °C): δ 168.2 (t, $J_{\text{F-F}}$ = 20.71 Hz, Zr–F), –49.3 (m, 2 F_{ortho}), –93.8 (t, $J_{\text{F-F}}$ = 18.8 Hz, 1 F_{para}), –98.8 (bs, 2 F_{meta}). ^{19}F NMR (THF- d_8 , –55 °C, aromatic fluorines): δ –51.5 (m, 1 F), –52.2 (m, 1 F), –96.9 (t, $J_{\text{F-F}}$ = 18.8 Hz, 1 F), –101.1 (m, 1 F), –101.8 (m, 1 F). Calcd for $\text{C}_{16}\text{H}_{10}\text{F}_6\text{Zr}$: C, 47.16; H, 2.47. Found: C, 46.99; H, 2.37. For Cp_2ZrF_2 , ^1H NMR (THF- d_8): δ 6.39 (s, 10 H). ^{19}F NMR (THF- d_8): δ 94.3. For $\text{C}_6\text{F}_5\text{H}$, ^1H NMR (THF- d_8): 7.34–7.45 (m). ^{19}F NMR (THF- d_8): δ –75.0 (m, 2 F), –91.1 (t, $J_{\text{F-F}}$ = 18.83 Hz, 1 F), –99.2 (m, 2F).

Thermolysis of $[\text{Cp}_2\text{ZrH}_2]_2$ with Pentafluorobenzene. A sample of $[\text{Cp}_2\text{ZrH}_2]_2$ (252 mg, 0.565 mmol) was suspended in 8 mL of THF. Pentafluorobenzene (13.5 mmol, 1.5 mL) was added at room temperature, and the mixture was heated to 65 °C. Within a few minutes vigorous gas evolution was observed and the suspension of $[\text{Cp}_2\text{ZrH}_2]_2$ disappeared to give a clear colorless solution. The solvent was removed to give a white powder (396 mg). A ^1H NMR spectrum of the sample revealed a 4:1 mixture of $\text{Cp}_2\text{Zr}(p\text{-C}_6\text{F}_4\text{H})\text{F}$ and Cp_2ZrF_2 . $\text{Cp}_2\text{Zr}(p\text{-C}_6\text{F}_4\text{H})\text{F}$ can be isolated by removing Cp_2ZrF_2 via sublimation (90 °C at 0.001 mmHg). An NMR tube scale reaction was performed at 65 °C with 23 mg (0.103 mmol based on monomer) of $[\text{Cp}_2\text{ZrH}_2]_2$ and $\text{C}_6\text{F}_5\text{H}$ (1.23 mmol, 137 μL) in THF- d_8 . Integration revealed a 4:1:2 mixture of $\text{Cp}_2\text{Zr}(2,3,5,6\text{-C}_6\text{HF}_4)\text{F}$, Cp_2ZrF_2 , and $p\text{-C}_6\text{F}_4\text{H}_2$, respectively. Hydrogen is also observed at δ 4.55 ppm. The formation of zirconium species was quantitative. For $\text{Cp}_2\text{Zr}(2,3,5,6\text{-C}_6\text{HF}_4)\text{F}$, ^1H NMR (THF- d_8): δ 7.027 (tt, $J_{\text{H-F}}$ = 9.4, 7.2 Hz), 6.40 (s, 10 H). ^{19}F NMR (THF- d_8 , 23 °C): δ 166.2 (t, $J_{\text{F-F}}$ = 18.8 Hz, Zr–F), –51.6 (bs, 2 F_{ortho}), –76.3 (bs, 2 F_{meta}). ^{19}F NMR (THF- d_8 , –70 °C, aromatic fluorines): δ –50.9 (m, 1 F), –51.4 (m, 1 F), –75.2 (m, 1 F), –76.5 (m, 1 F). Calcd for $\text{C}_{16}\text{H}_{11}\text{F}_5\text{Zr}$: C, 49.34; H, 2.85. Found: C, 49.43; H, 2.74. For $p\text{-C}_6\text{F}_4\text{H}_2$, ^1H NMR (THF- d_8): 7.40 (m, partially obscured by excess $\text{C}_6\text{F}_5\text{H}$). ^{19}F NMR (THF- d_8): δ –77.5 (s).

Reaction of $[\text{Cp}_2\text{ZrH}_2]_2$ with Various Concentrations of Perfluorobenzene. Three NMR tubes were prepared with varying concentrations of C_6F_6 (0.88, 1.78, and 2.68 M) in THF- d_8 . Each tube also contained 13 mg (0.029 mmol) of $[\text{Cp}_2\text{ZrH}_2]_2$ and α,α,α -trifluorotoluene as an internal standard. The NMR tubes were shaken vigorously for 20 s, put into the NMR spectrometer, and spun at 20 Hz. The reaction was followed by monitoring the growth of **1** via ^{19}F NMR spectroscopy at 23 °C until approximately half of the $[\text{Cp}_2\text{ZrH}_2]_2$ had disappeared. The products formed in each case were **1**, $\text{C}_6\text{F}_5\text{H}$, and Cp_2ZrF_2 in a ratio of 6:2:1. Hydrogen gas was also observed in each reaction but was not quantified. The rate of appearance of **1** was observed to be independent of the concentration of C_6F_6 . The relative ratios of the products was constant throughout the course of each reaction. A fourth NMR tube containing 13 mg of $[\text{Cp}_2\text{ZrH}_2]_2$ and 1.78 M C_6F_6 was also monitored without spinning. In this case the rate of appearance of **1** was approximately 50 times slower than those that were spun.

Reaction of $[\text{Cp}_2\text{ZrH}_2]_2$ and C_6F_6 with and without H_2 . Two NMR tubes were prepared with 13 mg (0.029 mmol) of $[\text{Cp}_2\text{ZrH}_2]_2$, C_6F_6 (1.78 M), and α,α,α -trifluorotoluene as an

(38) Chernega, A. N.; Graham, A. J.; Green, M. L. H.; Haggitt, J.; Lloyd, J.; Mehnert, C. P.; Metzler, N.; Souter, J. *J. Chem. Soc., Dalton Trans.* **1997**, 13, 2293.

(39) Wailes, P. C.; Weigold, H. *Inorg. Synth.* **1990**, 28, 257.

(40) Murphy, E. F.; Yu, P.; Dietrich, S.; Roesky, H. W.; Parisini, E.; Noltemeyer, M. *J. Chem. Soc., Dalton Trans.* **1996**, 1983.

(41) Brainina, E. M.; Dvoryantseva, G. G. *Izv. Akad. Nauk SSSR, Ser. Khim.* **1967**, 442.

(42) Chaudhari, M. A.; Stone, F. G. A. *J. Chem. Soc. (A)* **1966**, 838.

internal standard in THF- d_8 . To one tube was added approximately 4 atm of H_2 . The NMR tubes were shaken vigorously for 20 s and put into the NMR spectrometer and spun at 20 Hz. The reaction was followed by monitoring the growth of **1** via ^{19}F NMR spectroscopy at 23 °C until approximately half of the $[Cp_2ZrH_2]_2$ had disappeared. The products formed in each case were **1**, C_6F_5H , and Cp_2ZrF_2 in a ratio of 4:2:1. The rate of appearance of **1** was observed to be independent of the pressure of H_2 .

Reaction of $[Cp_2ZrH_2]_2$ with Pyridinium Poly(hydrogen fluoride). Pyridinium poly(hydrogen fluoride) (~30 wt % pyridine/70 wt % hydrogen fluoride) (~0.27 mmol HF) was added to a resealable NMR tube containing a THF- d_8 suspension of $[Cp_2ZrH_2]_2$ (15 mg, 0.067 mmol based on monomer). Vigorous gas evolution was observed immediately upon addition, and within a matter of seconds no $[Cp_2ZrH_2]_2$ remained. 1H and ^{19}F NMR spectroscopy revealed Cp_2ZrF_2 as the only metal-containing compound. Hydrogen gas was also observed in the 1H NMR spectrum. A similar reaction was performed with ~0.13 mmol of pyridinium poly(hydrogen fluoride). In this case only half of the $[Cp_2ZrH_2]_2$ was converted to Cp_2ZrF_2 ; the remainder was left as an unreacted solid in the NMR tube.

Reaction of Cp_4Zr with Pyridinium Poly(hydrogen fluoride). Pyridinium poly(hydrogen fluoride) (~30 wt % pyridine/70 wt % hydrogen fluoride) (~0.025 mmol HF) was added to a resealable NMR tube containing a THF- d_8 solution of Cp_4Zr (18 mg, 0.05 mmol) at room temperature. 1H and ^{19}F NMR spectroscopy revealed cyclopentadiene, Cp_3ZrF , and Cp_2ZrF_2 , the latter two in a ratio of ~1.8:1. For Cp_3ZrF , 1H NMR (THF- d_8): δ 6.099 (s). ^{19}F NMR (THF- d_8): δ 25.5 (s, Zr-F). MS (70 eV, direct inlet, 300 °C): m/e 304 (M^+), 285 ($M^+ - F$), 239 ($M^+ - Cp$), 220 ($M^+ - Cp - F$), 174 ($M^+ - 2Cp$).

Reaction of Cp_3ZrH with Various Concentrations of C_6F_6 . A 0.06 M THF- d_8 stock solution of Cp_3ZrH containing hexamethylbenzene as an internal standard was prepared, and 0.4 mL aliquots were added to three resealable NMR tubes. Perfluorobenzene (30, 60, and 90 μ L) was added to each NMR tube. The volume of each tube was adjusted to 0.91 mL by addition of THF- d_8 , giving a concentration of Cp_3ZrH of 0.026 M and concentrations of perfluorobenzene of 0.29, 0.57, and 0.86 M. The NMR tubes were stirred at room temperature, and the reaction was followed by 1H NMR spectroscopy for three half-lives. The products of the reaction were **1**, CpH , C_6F_5H , Cp_2ZrF_2 , Cp_4Zr , Cp_3ZrF , and Cp_3ZrX , in a 3.8:3.8:2.7:1.0:0.77:0.74:0.62 ratio. A plot of $\ln[Cp_3ZrH]$ vs time was linear. The observed pseudo-first-order rate constants were $2.22(3) \times 10^{-6} s^{-1}$ (0.29 M), $4.40(16) \times 10^{-6} s^{-1}$ (0.57 M), and $6.19(12) \times 10^{-6} s^{-1}$ (0.86 M).

Reaction of Cp_3ZrH (2) with C_6F_6 and TBAF. A 0.06 M THF- d_8 stock solution of Cp_3ZrH containing hexamethylbenzene as an internal standard was prepared, and a 0.4 mL aliquot was added to a resealable NMR tube. Perfluorobenzene (60 μ L) was added to the NMR tube. A benzene solution of TBAF was added to give a 0.8 M solution in TBAF. The sample was diluted with THF- d_8 to 0.91 mL, giving a solution of Cp_3ZrH (0.026 M) and perfluorobenzene (0.57 M). The NMR tube was stirred at room temperature, and the reaction was followed by 1H NMR spectroscopy for three half-lives. There was no rate acceleration for the disappearance of **2** compared to the reaction without TBAF, although the main organometallic product was now Cp_2ZrF_2 ; only a trace of $Cp_2Zr(C_6F_5)F$ was observed.

X-ray Structural Determination of **1 and **2**.** A colorless crystal approximately $0.38 \times 0.18 \times 0.12$ mm³ of **1** was mounted on a glass fiber under Paratone-8277 (Exxon) and immediately placed in a cold nitrogen stream at -80 °C on the X-ray diffractometer. A very small colorless plate of **2** ($0.24 \times 0.01 \times 0.01$ mm³) was mounted in the same manner, and the data were also obtained at -80 °C. The X-ray intensity data for the two crystals were collected on a standard Siemens SMART CCD area detector system equipped with a normal

Table 1. Crystallographic Data for $Cp_2Zr(C_6F_5)F$ (1**) and Cp_3ZrH (**2**)**

	1	2
Crystal Parameters		
chemical formula	$C_{16}H_{10}F_6Zr$	$C_{15}H_{16}Zr$
fw	407.46	287.50
cryst syst	orthorhombic	hexagonal
space group	$Pna2_1$	$P6_3/m$
Z	4	2
a , Å	15.772(3)	8.0122(6)
b , Å	11.408(3)	8.0122(6)
c , Å	7.8990(7)	10.3314(11)
vol, Å ³	1421.2(4)	574.37(9)
ρ_{calc} , g cm ⁻³	1.904	1.662
cryst dims, mm ³	$0.12 \times 0.18 \times 0.38$	$0.01 \times 0.01 \times 0.24$
temp, °C	-80	-80
Measurement of Intensity Data		
diffractometer	Siemens SMART	Siemens SMART
radiation	Mo, 0.71073 Å	Mo, 0.71073
frame range/time, deg/s	0.3/30	0.3/60
2θ range, deg	4.4–56.6	5.9–46.4
data collected	$-10 \leq h \leq 20$, $-13 \leq k \leq 14$, $-10 \leq l \leq 10$	$-8 \leq h \leq 6$, $-7 \leq k \leq 8$, $-11 \leq l \leq 11$
no. of data collected	8420	2526
no. of unique data	3281	298
no. of obs data ($I > 2\sigma(I)$)	2757	288
agreement between equivalent data (R_{int})	0.0368	0.0400
no. of params varied	208	42
μ , mm ⁻¹	0.836	0.924
systematic absences	$0kl, k+l$ odd, $h0l, h$ odd; $00l, l$ odd	$00l, l$ odd
abs corr	empirical (SADABS)	empirical (SADABS)
range of trans factors	0.605–0.928	0.714–0.928
$R1(F_o)$, $wR2(F_o^2)$ ($I > 2\sigma$)	0.0307, 0.0607	0.0313, 0.0589
$R1(F_o)$, $wR2(F_o^2)$ (all data)	0.0415, 0.0640	0.0352, 0.0602
goodness of fit	0.961	1.317
absolute structure param	-0.05(4)	

focus molybdenum-target X-ray tube operated at 2.0 kW (50 kV, 40 mA). A total of 1321 frames of data (1.3 hemispheres) were collected using a narrow frame method with scan widths of 0.3° in ω and exposure times of 30 s/frame for **1** and 60 s/frame for **2** using a detector-to-crystal distance of 5.094 cm (maximum 2θ angle of 56.52°). The total data collection time was approximately 13 h for 30 s exposures and 26 h for 60 s exposures. Frames for **1** were integrated to 0.75 Å with the Siemens SAINT program to yield a total of 8420 (3281 independent) reflections. Frames for **2** were integrated to 0.90 Å, yielding 2526 (298 independent) reflections. Laue symmetry revealed an orthorhombic crystal system for **1** and a hexagonal crystal system for **2**. The final unit cell parameters (at -80 °C) were determined from the least-squares refinement of three-dimensional centroids of 4856 reflections for **1** and 1706 reflections for **2**.⁴³ Data were corrected for absorption using the program SADABS.⁴⁴ The space groups for **1** and **2** were assigned as $Pna2_1$ (No. 33) and $P6_3/m$ (No. 176), respectively. The structure solutions were achieved by direct methods and refined employing full-matrix least-squares on F^2 (Siemens, SHELXTL,⁴⁵ version 5.04). One independent molecule was located in the asymmetric unit for **1**, as expected for $Z =$

(43) It has been noted that the integration program SAINT produces cell constant errors that are unreasonably small, since systematic error is not included. More reasonable errors might be estimated at 10× the listed value.

(44) The SADABS program is based on the method of Blessing; see: Blessing, R. H. *Acta Crystallogr., Sect. A* **1995**, *51*, 33.

4. All of the atoms were refined anisotropically, with hydrogens included in idealized positions, and the structure was refined to a goodness of fit (GOF)⁴⁶ of 0.965 and final residuals⁴⁷ of $R1 = 3.07\%$ ($I > 2\sigma(I)$), $wR2 = 6.07\%$ ($I > 2\sigma(I)$). For a $Z = 2$, one-sixth of the molecule was located in the asymmetric unit of **2**. The Zr and hydride atoms were found to be disordered across the mirror plane, and successful anisotropic refinement was achieved as described in the text. The hydrogen atoms were located, and their positions and isotropic thermal pa-

rameters were refined. The structure refined to a goodness of fit (GOF)⁴ of 1.318 and final residuals⁵ of $R1 = 3.13\%$ ($I > 2\sigma(I)$), $wR2 = 5.90\%$ ($I > 2\sigma(I)$). Data collection and refinement parameters are listed in Table 1.

Acknowledgment. Acknowledgment is made to the U.S. Department of Energy, Grant FG02-86ER13569, for their support of this work.

Supporting Information Available: Tables of bond distances and angles and atomic positions for **1** and **2**. This material is available free of charge via the Internet at <http://pubs.acs.org>.

OM9902481

(45) *SHELXTL: Structure Analysis Program, version 5.04*; Siemens Industrial Automation Inc.: Madison, WI, 1995.

(46) $GOF = [\sum(w(F_o^2 - F_c^2)^2)/(n - p)]^{1/2}$, where n and p denote the number of data and parameters.

(47) $R1 = (\sum||F_c| - |F_o||)/\sum F_o$; $wR2 = [\sum[w(F_o^2 - F_c^2)^2]/\sum[w(F_o^2)^2]]^{1/2}$, where $w = 1/[\sigma(F_o^2) + (aP)^2 + bP]$ and $P = [(\max(0, F_o^2) + 2F_c^2)/3]$.